Physical and Dynamical Processes At and Above Severe Thunderstorms

Pao K. Wang
Department of Atmospheric and Oceanic Sciences
University of Wisconsin-Madison
1225 W. Dayton Street
Madison, WI 53706
USA

1. Introduction

Cloud top processes are important to satellite observations of weather phenomena because they produce cloud features that are directly observable. Two main cloud top phenomena will be discussed in this paper, namely, the anvil top plumes and the cloud top temperature field, both are referring to the severe thunderstorm conditions.

Regarding the cloud top plume phenomenon, recently Setvak and Doswell (1991) and Levizzani and Setvak (1996) reported the observation of plume-like features on top of some convective storms using the Advanced Very High Resolution Radiometer (AVHRR) satellite imageries of the US National Oceanographic and Atmospheric Administration (NOAA) polar orbiters. The physical mechanism for this phenomenon is unclear at present. Aside from pure scientific curiosity, studying this phenomenon can yield some practical benefits as well. For instance, since it is normally difficult, even hazardous, to make in situ observations above a severe thunderstorm, remote observation of such phenomena may be utilized to our benefit to understand cloud top physical and dynamical processes if it can be properly interpreted. As it turns out from hindsight, this phenomenon may even be of some important implications to the global transport of water vapor, especially in the area of stratospheric-tropospheric exchange (STE).

In this paper, I would like to offer an explanation for the possible mechanisms responsible for this plume phenomenon. I will use the numerical cloud model simulation results of a High Plains supercell storm to illustrate the explanation

Secondly, the cloud top temperature field as observed by satellite IR images has been discussed by many investigators and summarized by Heymsfield and Blackmer (1988). The same model results as mention above can also be used to explain the important characteristics of the temperature field.

2. Observed Characteristics of the Plumes

The following list of the plume characteristics is compiled from the articles of Setvak and Doswell (1991) and Levizzani and Setvak (1996) whose studies were based mainly on the NOAA/AVHRR imagery channel 2 (0.625-1.1 μm), channel 3 (3.55-3.93 μm), and channel 4 (10.3-11.3 μm). Thus these are characteristics in infrared channels although the visible channel (channel 1) characteristics are also included. While the plumes studied by these investigators were all taken from thunderstorms occurred in Europe, there is no reason to suspect their existence in the convective storms of North America or other midlatitude regions. Some of the characteristics listed below are common to all plumes whereas others are true only to specific cases:

(a) A small bright spot in channel 2 (the size of a few pixels, i.e., a few km) in the form of an oval cloud is detected as the plume's source. The shadow cast by this rounded cloud appears much longer than that of the plume, suggesting a higher altitude.
(b) The source spot is normally shifted downwind from the coldest area and in the storm's embedded warm area.
(c) The plumes spread downwind resembling plumes from a chimney. The estimated height is usually about 15 km.
(d) They are vertically separated from the underlying anvils. This is deduced from the shadows they cast on the anvils.
(e) Plumes are partially transparent in channel 1 and 2.
(f) The structure of the plume is more or less preserved in channel 4, indicating a temperature difference between the particles of the plume and the surroundings.
(g) Sometimes the plume splits into two very bright splinters with *cyclonic* curvature for the northern branch and *anticyclonic* for the southern branch. The source of the split plume appears to be in the distant warm area. The northern branch is estimated to be about 50 m above the anvil.
(h) The plumes can be quite long. Sometimes they are as long as or even longer than the anvils.

The terms "embedded warm area" and "distant warm area" refer to the features of cloud top temperature fields above some severe thunderstorms as discussed by Heymsfield and Blackmer (1988).

3. Hypothesis of the plume formation mechanisms

Since the plumes are visible (albeit semi-transparent) in channel 1, they most likely are composed of condensed form of water substance, either liquid droplets or ice particles. This requires that water vapor be transported from the troposphere to the stratosphere through the tropopause. The point-like source of the plumes observed for all cases helps to narrow down the choices of possible mechanisms. The two natural choices for the water vapor transport are: (1) the overshooting connected with the updraft core and (2) the breaking of gravity waves on the cloud top.

Our study suggests that the plume generation mechanism is the gravity waves near the cloud top of a severe thunderstorm. As indicated above, the cloud top surface, which roughly coincides with the tropopause, behaves like a material surface with a stable stratification above it, gravity waves can be generated by the strong convective disturbance (Houze, 1993). The mostly likely mechanism that is related to the plume formation is the breaking of the wave crests, a mechanism similar to water drops formed above breaking waves on ocean surface due to jet instability. The typical dimension of breaking wave is about a few kilometers. While not completely ruling out the possibility of transport by the updrafts in the overshooting region, it appears that the main process responsible for the formation of plume is the breaking of gravity waves.

In the following section, the results of a model simulation of a Midwest supercell storm are used to illustrate this process.

4. Numerical simulation of the 2 August 1981 CCOPE supercell storm

The cloud model used for performing the simulation is the Wisconsin Dynamical/Microphysical Model (WISCDYMM). This is a 3-dimensional nonhydrostatic primitive equation model cast in quasi-compressible form. Turbulent fluxes are approximated by the one-and-a-half order closure theory of Klemp and Wilhelmson (1978). The thermodynamic equation with potential temperature as the dependent variable follows the approximation given by Das (1969).

The cloud microphysical processes include the conversion and interactions among water vapor and five classes of hydrometeors (cloud water, cloud ice, rain, snow, and graupel/hail). The model can be run in the bin mode for a specific class of hydrometeors (say, graupel/hail) if desired. In the present study, bulk parameterizations of microphysical processes are used. The expressions of the parameterizations are taken from Lin et al. (1983), Farley et al. (1986), and Farley (1987a, b). More details of the model and its parameterizations are given in Straka (1989).

The storm simulated here is the 2 August 1981 supercell, which passed through the Cooperative Convective Precipitation Experiment (CCOPE) in southern Montana (Knight 1982; Miller et al. 1988). This case is merely used as an example to demonstrate that plumes could have been formed in a typical severe thunderstorm such as this. Many instruments have observed the storm and hence there are extensive data sets that can be used to verify model results. Other than these, there is nothing unique about this storm.

5. Results and discussions

Since the main microphysical and dynamical features are the same as that in Johnson et al. (1993, 1994), only the results that are relevant to the plume formation will be presented here. The main variables that we are interested to examine here are the relative humidity with respect to ice (RHi) and water vapor mixing ratio (qv). The profiles of these two variables have not been examined before and their distributions above the anvil have direct bearing to the plumes.

The results of the simulation do *not* show any condensed-water plume formation. The reason why no such plume formed in this simulation is most likely due to the very dry upper-air environment prescribed in the initial conditions (no water vapor at all above 300 mb) as noted in the previous section. But the RHi and qv profiles show plume-like features and strongly suggest that the plumes could have formed under proper conditions. In addition, the characteristics of the vapor plumes are striking similar to the observed plumes. The properties of these vapor plumes are the subject of the following discussions.

One of the most prominent features in the cloud top region, as deduced from the simulation results, is the violent perturbation related to the storm-generated gravity waves. It appears that these gravity waves are the most important mechanism that produces the plumes. The animations of either the RHi or qv profiles reveal most easily the gravity wave phenomenon, but unfortunately they cannot be shown here. In the following, some snapshots are provided to illustrate this phenomenon and the related mechanism of plume formation.

Figure 1 shows a series of snapshots of vertical profiles of RHi at the central vertical x-z plane at y = 50 km for t = 16, 20, 24, 40, 80, and 90 min. The red area outlines roughly the core of the supercell storm. The reason to examine the RHi instead of the relative humidity with respect to water is because we are mainly interested in the cloud top region where most of the hydrometeors formed are ice particles.

Figure 1(a) shows the RHi profile of the simulated storm at t = 16 min. This is the first time that a jet-like feature, the precursor of the plume, occurs at the point at the cloud top (x = 60, z = 13.75). This point is not located at the highest point of the overshooting, rather it occurs at the point where rapid updrafts change into rapid downdrafts, in other words, strong shear. It looks like water drops produced at the top of a breaking water wave.

The other panels show the subsequent stages of the plume development. The small jet in figure 1(a) has gradually developed into an extended patch of humid air with a core RHi that can be greater than 80%. The height of the patch center is at about z = 15 km, close to that observed for the plumes. In addition to this patch, there is another high RHi area further downstream that is produced by the upwelling of a wave crest. The storm reaches steady state at about 80 min (figure 1(e)) and the humid air patch above the anvil start to take the shape of a plume, centered at z = 15 km. At 90 min the plume structure is more of the same as at 80 min. The vapor plume becomes thinner at later stages but is always present to the end of the simulated period (t = 150 min). The height of this vapor plume seems to be at about the same level as observed by Levizzani and Setvak (1996) [Point (c) in Sec. 2]. Note that these figures show only the central vertical cross-section of the RHi field and hence do not show the full length of the plumes since the plumes are not aligned completely along this cross-section.

6. Cloud top temperature field

Heysmsfield and Blackmer (1988) described the satellite IR cloud top temperature field above a severe thunderstorm with the following three distinct features: (1) a cold V or U near the front edge of the storm; (2) a closed-in warm area; and (3) a distant warm area. The model results show that the formation of these features van be explained mainly by the adiabatic dynamical processes. The details of the study will be presented in the meeting.

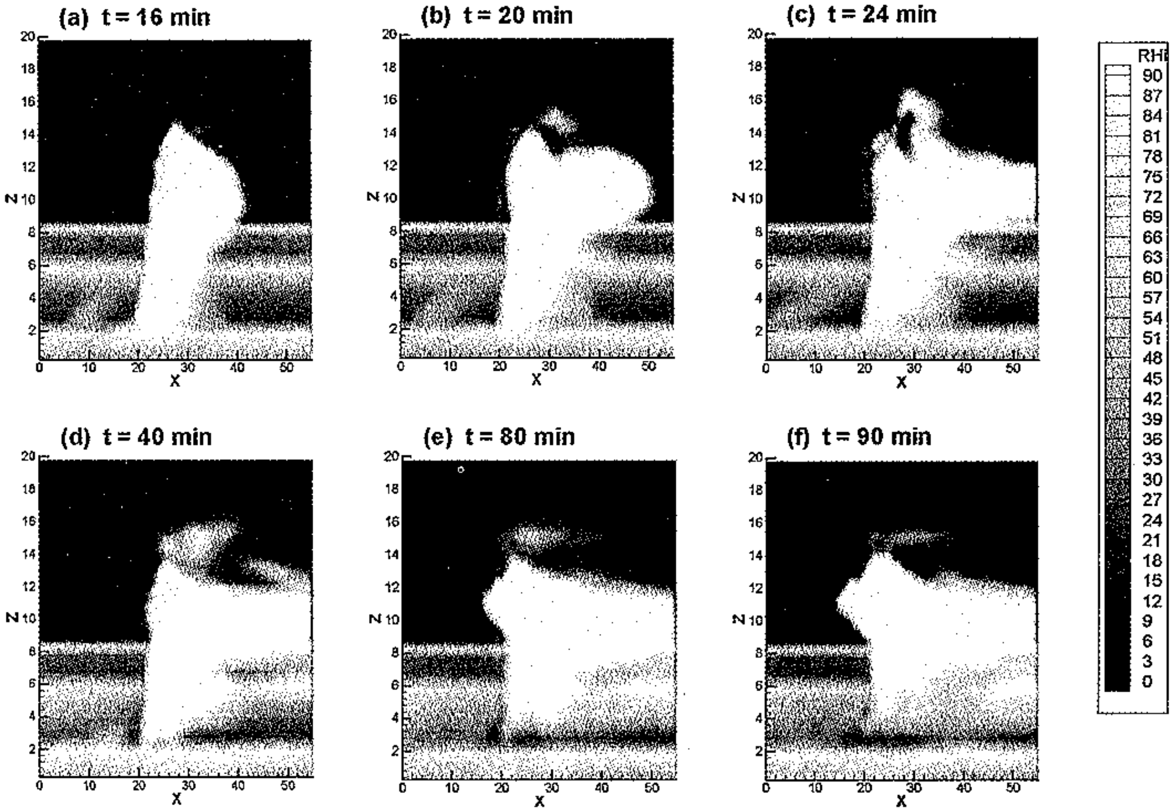

Figure 1. Snapshots of vertical profiles of RHi at the central vertical x-z plane at y = 50 km for t = 16, 20, 24, 40, 80, and 90 min.

Acknowledgments. This work is partially supported by NSF grants ATM-9633424, ATM-9714158, and ATM-9907761. The author thanks H. M. Lin and Y. L. Chu for helping the processing of model data.

References

Das, P., 1969: The thermodynamic equation in cumulus dynamics. *J. Atmos. Sci.*, **26**, 399-407.

Farley, R. D., 1987a: Numerical modeling of hailstorms and hailstone growth. Part II:The role of low-density riming growth in hail production. *J. Climate Appl. Meteor.*, **26**, 234-254.

Farley, R. D., 1987b: Numerical modeling of hailstorms and hailstone growth. Part III: Simulation of an Alberta hailstorm-Natural and seeded cases. *J. Climate Appl. Meteor.*, **26**, 789-812.

Farley, R. D., and H. D. Orville, 1986: Numerical modeling of hailstorms and hailstone growth. Part I: Preliminary model verification and sensitivity test. *J. Climate Appl. Meteor.*, **25**, 2014-2036.

Goody, R. M., and Y. L. Yung, 1989: *Atmospheric Radiation: Theoretical Basis.* 2nd ed., Oxford University Press, New York, 519pp.

Heymsfield, G. M., and R. H. Blackmer, Jr., 1988: Satellite-observed characteristics of Midwest severe thunderstorm anvils. *Mon. Wea. Rev.*, **116**, 2200-2224.

Holton, J. R., P. H. Haynes, M. E. McIntyre, A. R. Douglass, R. B. Rood, and L. Pfister, 1995: Stratospheric-tropospheric exchange. *Rev. Geophys.*, **33**, 403-439.

simulation of the 2 August 1981 CCOPE supercell storm with and without ice microphysics. *J. Appl. Meteor.*, **32**, 745-759.

Johnson, D. E., and P. K. Wang, and J. M. Straka, 1995: A study of microphysical processes in the 2 August 1981 CCOPE supercell storm. *Atmos. Res.* **33**, 93-123.

Klemp, J. B., and R. B. Wilhelmson, 1978a: The simulation of three-dimensional convective storm dynamics. *J. Atmos. Sci.*, **35**, 1070-1096.

Klemp, J. B., and R. B. Wilhelmson,1978b: Simulations of right- and left-moving storms produced through storm-splitting. *J. Atmos. Sci.*, **35**, 1087-1110.

LevizzaniV., and M. Setvak, 1996: Multispectral, high resolution satellite observations of plumes on top of convective storms. *J. Atmos. Sci.*, **53**, 361-369.

Lin, Y. L., R. D. Farley, and H. D. Orville, 1983: Bulk parameterization of the snow field in a cloud model. *J. Climate Appl. Meteor.*, **22**, 1065-1092.

Houze, Jr., R. A., 1993: *Cloud Dynamics*. Academic Press, New York, 570pp.

Johnson, D. E., P. K. Wang, and J. M. Straka, 1993: Numerical

Matsuno, T., 1966: Numerical integrations of the primitive equations by a simulated backward difference method. *J. Meteor. Soc. Japan*, **44**, 76-83.

Miller, L. J., D. Tuttle, and C. A. Knight, 1988: Airflow and hail growth in a severe northern High Palins supercell. *J. Atmos. Sci.*, **45**, 736-762.

Setvak, M. and C. A. Doswell III, 1991: The AVHRR channel 3 cloud top reflectivity of convective storms. *Mon. Wea. Rev.*, **119**, 841-847.

Sharman, R. D., and M. G. Wurtele, 1983: Ship waves and lee waves. *J. Atmos. Sci.*, **40**, 396-427.

Straka, J. M., 1989: *Hail growth in a highly glaciated central high plains multi-cellular hailstorm.* Ph.D thesis, University of Wisocnsin-Madison, 413pp.

Wang, P. K., 2000: An interpretation of the cloud top temperature signature of Midwest severe thunderstorms. (Under preparation)